https://dx.doi.org/10.4314/dujopas.v10i1b.1
ISSN (Print): 2476-8316
ISSN (Online): 2635-3490
Dutse Journal of Pure and Applied Sciences (DUJOPAS), *Vol. 10 No. 1b March 2024*

Charge Transport Enhancement in Some Acene-Based Molecular Junctions

Kassim L. Ibrahim[1*], G. Babaji[2] and G.S.M. Galadanchi[2]

[1]Lecturer, Physics Department,
Kano University of Science and Technology,
Wudil, Kano, Nigeria.
Orcid ID: 0009-0005-8803-5500

[2]Bayero University Kano,
Nigeria

Email: ikassim27@gmail.com

Abstract

The field of single molecule electronics research has been spurred by the need to add functionality to next-generation electronic circuits and the desire to miniaturize devices. We focused on some acene-based molecular junctions, in which molecules are connected to Au electrodes via anchor groups. The frontier molecular orbitals (FMOs) and charge transport nature of the junction were examined by employing the density functional theory (DFT) in conjunction with the non-equilibrium Green's functional (NEGF) formalism. Particular attention was paid to the anchoring groups (NH_2, S, CN, and SH), chemical impurity doping (B, N, and NB), and side groups (-CH_3, -NH_2, and –NO_2). The findings demonstrate that the FMOs can change depending on the dopants or substituents employed. Additionally, it is noted that depending on the materials employed, charge transfer may be p-type or n-type. It is discovered that the molecular junctions have the highest conductivity when cyanides are used as anchor groups. It is therefore the ideal anchor material to utilize with tetracene and pentacene molecules. Understanding and creating n-type or p-typed high conductivity single molecule electronic components can be greatly aided by these discoveries.

Keywords: Acenes, DFT, HOMO-LUMO, NEGF, Transmission

INTRODUCTION

Carbon-hydrogen bonds make up substances that are classified as organic. By adding chemical groups, these materials' electrical properties can be altered, and their structural features can be changed. Additionally, they are mechanically flexible, and their production processes are easy, affordable, and available. Due to their dielectric nature, almost all organic materials have long been utilized as electrical insulators (Aviram and Ratner, 1974). These molecules have π-bonds in common, and their semiconducting qualities result from electrons hopping between π-orbitals. As such, these materials have a good reputation in applications related to electronics (Aadhityan, *et al.,* 2020). Thus, there's hope that they can eventually replace conventional silicon semiconductors. Due to the fact that silicon-based electronic device downsizing is reaching its physical limits, single-molecule electronic devices have caught significant attention lately (Cheng *et al.,* 2020). These investigations demonstrate that a variety of the molecule-structures, anchoring groups, and electrode materials, are important in molecular electron transport. The field of molecular electronics is one such technology that

**Author for Correspondence*

can enable high integration densities and low power consumption (Sirohi, *et al.,* 2021). The ultimate goals of molecular electronics are the miniaturization of electronic devices and the integration of functional molecular devices into circuits.

Michael and Ferdinand (2018) state that among the most important architectures in the field of molecular nanostructures is a molecular junction (MJ). In this structure, a single molecule is bound to metal or semiconductor electrode clusters. This field of study has seen significant advancements in recent years and is an extremely active area of experimental and theoretical research. An anchoring group is put in place to connect the single-molecule to two electrodes (see Figure 2). By applying the fundamentals of non-equilibrium many-body quantum physics at the nanoscale, the main goals of MJs are to develop technological applications in molecular nano-electronic devices.

Acenes are polycyclic aromatic hydrocarbon, a subclass of organic semiconductors formed out of several adjacent benzene rings organized in a row. Due to the instability of large acenes, these attempts have, unfortunately, not been very successful. Therefore, there has been a recent surge in interest in studying small acenes, such as anthracene (Ibrahim *et al.,* 2022), tetracene (Yelin *et al.,* 2021), and pentacene (Pinheiro *et al.,* 2020). To this end, some theoretical and experimental attempts have been made to assess the effect of substituting hydrogen with different chemical groups (Akbarabadi *et al.,* 2021; Wang *et al.,* 2020; He *et al.,* 2020; Chen *et al.,* 2020; Ramezani *et al.,* 2021).

METHODOLOGY

This work involves the extended structure modeling, density functional theory (DFT) calculations, and nonequilibrium Green's function (NEGF) formalism simulations. Jmol and FHI-aims computer algorithms were used for the structure modeling and optimization, respectively. The Au electrodes (leads/reservoirs) in all of our constructions are coupled in para locations (Stegmann *et al.,* 2020). The Perdew-Burke-Ernzerhof (PBE) exchange correlation functional was used in DFT calculations as implemented in the FHI-aims computer program (Blum *et al.,* 2009). Meanwhile, the transport properties of the system were examined using the NEGF approach as implemented in the Aitranss computer code (Arnold, *et al.,* 2007; Wilhelm, *et al.,* 2013 and Bagrets, 2013).

This work's initial step was examining the effects of various anchoring groups. This is done in order to determine which anchor material best fits the desired electrical conductivity property. Amine (NH_2), cyanide (CN), sulfur (S), and thiol (SH) are the constituents employed for this task. The connection between electrodes and molecules via anchoring group is at para positions is shown in Figure 1. Using the impurity doping approach (Akbarabadi *et al.,* 2020), the conductance of the MJ was examined in the second phase. Since boron (B) and nitrogen are the most widely utilized dopants for carbon-based materials, we choose them as the primary dopants in this phase (Blanca and Blase 2009). An investigation was conducted into the effects of side-groups (Yuan, *et al.,* 2021) on the charge transport of the MJs. Here, three distinct side-groups, nitro (NO_2), amine (NH_2), and methyl (CH_3), were studied while preserving the structure's symmetry (Akbarabadi *et al.,* 2021).

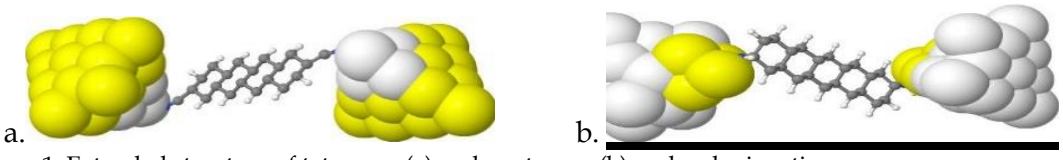

Figure 1: Extended structure of tetracene (a) and pentacene (b) molecular junctions

The transport properties of the structures are calculated via the Landauer-Buttiker formalism defined by the Green's function in equation (1) by Ali *et al.,* 2017;

$$G(E) = [ES - H_C - \sum_L(E) - \sum_R E]^{-1} \quad (1)$$

Where E is the energy, H_c is the Hamiltonian, and S is the overlap matrix corresponding to the scattering region, while $\sum_{L/R}(E)$ are the self-energies of the left and right electrodes.
The electrical conductance is related to the transmission coefficient through the Landauer formular (Cheng *et al.,* 2020);

$$G = \left(\frac{2e^2}{h}\right) \int_{-\infty}^{\infty} T(E) \left(\frac{\partial f(E,T)}{\partial E}\right) dE \quad (2)$$

Where $f(E,T)$ is the distribution function given as $f(E,T) = \left[e^{(E-E_f)/k_BT} + 1\right]^{-1}$ with k_B a Boltzmann's constant and E_f is the Fermi energy of the electrodes.

RESULTS AND DISCUSSION

Anchoring Groups: Here, several anchoring groups link the molecules of tetracene, and pentacene to the Au-electrodes. The kind of transport in the MJ can be classified as p-type (HOMO-dominated) or n-type (LUMO-dominated) depending on the choice of anchoring groups.

Tetracene: The effects of various anchoring groups on tetracene molecules when coupled to Au-electrodes are depicted in Figure 2 below. In the case of prestine (Figure 2a.), the HOMO is localized on the tetracene molecule and is considered as control in checking the effects of anchoring group on tetracene molecules. In the case of amines anchoring group, the transport may likely occur in the HOMO level, as the energy is slightly localized on the HOMO transportation path (Figure 2b.). In the case of cyanides anchoring group, (c and h), HOMO and LUMO are much similar, resulting in the transportation due to contribution of both. In contrast, for sulphides (d and i), the LUMO is totally localized on the sulphur atom. HOMO, on the other hand, is dispersed across the expanded molecule and, in this instance, dominates the transport. Finally, the thiols had an impact on the tetracene molecule, causing the LUMO to be slightly more concentrated on the anchoring group than the HOMO and possibly leading to a LUMO-dominated transport.

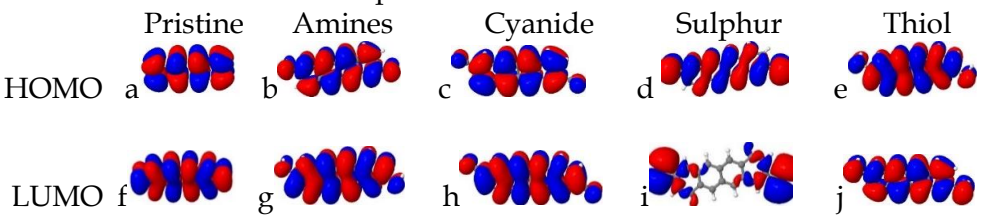

Figure 2: Frontier molecular orbitals for tetracene molecules connected to Au electrodes through four different anchoring groups.

Table 1: HOMO and LUMO variation with different anchor groups in tetracene MJs

Anchor material	HOMO (eV)	LUMO (eV)	HOMO-LUMO gap(eV)
Prestine	-4.7245	-4.7179	0.0066
Amines	-4.6957	-4.6108	0.0849
Cyanides	-4.6541	-4.6355	0.0186
Sulphides	-4.8928	-4.8495	0.0433
Thiols	-4.6820	-4.5850	0.0970

It is evident from Table 1 that the anchoring group raises the HOMO-LUMO gap's value. As can be observed, when anchor groups are attached, the gap for the prestine situation is smaller than those values. This indicates that when tetracene molecules are joined to anchor materials, they become less excited.

The transmission coefficients of tetracene molecules with various anchoring groups plotted against energy are shown in Figure 3. In this instance, the electrical conductance value is increased by the anchoring group. Cyanides (blue) have a neutral transport character and the highest transmission coefficient T(E) at E_F of 0.8703. Because the amines anchoring group's (green) HOMO energy is closer to Fermi energy (E_F), it exhibits HOMO-dominated (p-type) transport with a transmission coefficient of 0.5853. Sulfides similarly have a transmission coefficient of 0.3422 for p-type (HOMO-dominated) transport. The least transmission coefficient, 0.2335, is exhibited by thiols, who have LUMO-dominated (n-type) transport. These results are in agreement with the work by Balachandran, *et al.,* (2012).

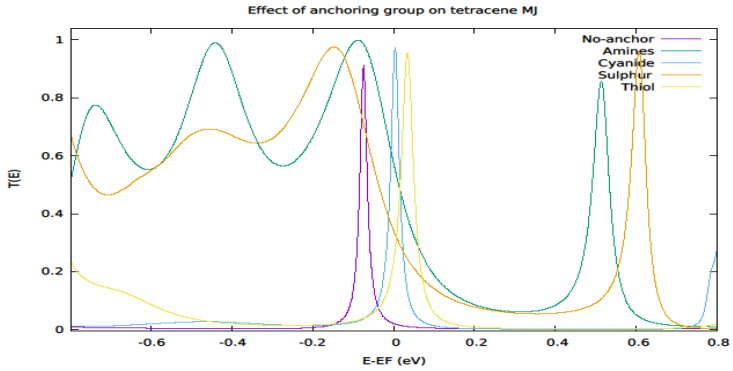

Figure 3: Transmission coefficients of tetracene molecules versus energy, a comparison when connected to electrode through different anchor groups.

Pentacene MJs: Pentacene molecules are connected to Au electrodes using four distinct anchoring groups in this instance as well. The border molecular orbitals shown in Figures 4a and e represent the prestine arrangement, or pentacene without an anchoring group, which will be used as a control to see how an anchoring group affects the electrical conductivity of pentacene molecular jewels. This figure illustrates how the LUMO (e) is not localized and the HOMO-LUMO gap is 0.0599 eV for the prestine (a), whereas the HOMO is confined within the pentacene molecule. Since the energy pattern of the pentacene MJs does not significantly alter from the prestine case, the effects of amines (b and f), cyanides (c and g), and thiols (d and i) are minimal. The HOMO-LUMO gap to 0.0556, 0.0, and 0.0183 eV, in that order. Accordingly, the pentacene MJs' excitation ability is increased by the amine and cyanides and decreased by the thiols. On the other hand, sulfur dioxide physically affects pentacene MJs' HOMO and LUMO and closes the HOMO-LUMO gap to 0.0073 eV.

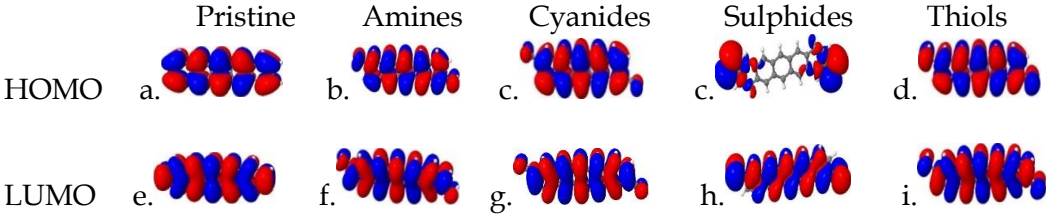

Figure 4: Frontier molecular orbitals for pentacene molecules connected to Au electrodes through four different anchoring groups.

Table 2: HOMO and LUMO variation on pentacene MJs with different anchor groups

Anchor material	HOMO (eV)	LUMO (eV)	HOMO-LUMO gap(eV)
Pristine (H)	-4.4953	-4.4354	0.0599
Amines (NH_2)	-4.6035	-4.5852	0.0183
Cyanides (CN)	-4.7268	-4.6712	0.0556
Sulphides (S)	-4.8245	-4.8172	0.0073
Thiol (SH)	-4.4977	-4.0649	0.4328

Table 2 indicated that, apart from thiol, all other anchoring group reduces the value of HOMO-LUMO gap (increases excitation), with sulphides having the least gap.

The results of the transport calculation on the pentacene MJs are displayed in Figure 5, along with the impact of anchoring groups on the transmission coefficients T(E) against energy. When compared to anthracene and tetracene MJs, the T(E) of a pentacene MJ without an anchoring group at the Fermi energy level is 0.07066, which is significantly less. The T(E) value increases to 0.1267 when an amines anchor is utilized, and its HOMO approaches Fermi energy (p-type transportation). Moreover, sulphides have p-type, HOMO-dominated transport with a T(E) value of 0.2734. Conversely, the T(E) values of cyanides and thiols are 0.3757 and 0.01483, respectively, and their LUMO is closer to the Fermi energy.

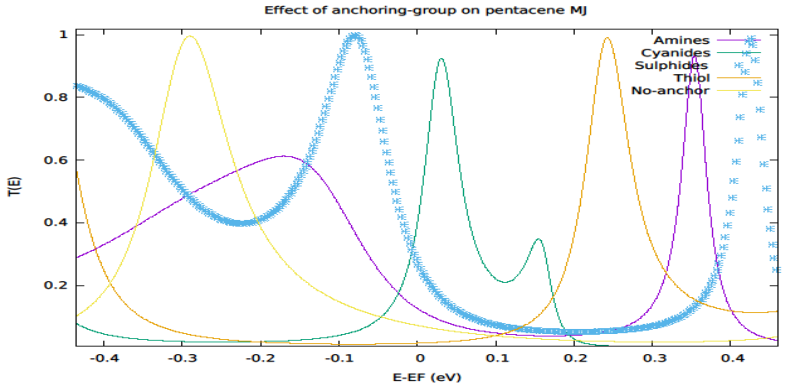

Figure 5: Transmission coefficients of pentacene molecules versus energy

Additionally, these findings somewhat concur with those of Balachandran *et al.* (2012) and Fujii *et al.* (2020).

Doping: Boron (B) and Nitrogen (N) are the main dopants commonly used for carbon-based materials (Blanca and Blaze, 2009). A single carbon substitution by B and N, and a double carbon substitutions by N and B atoms at the edge of the middle benzene ring of the simple geometry of an acene molecules (i.e, scattering region of the MJ).

Tetracene: A cyanides was used as an anchoring group the entire time in this section. According to Figure 6, in the case of a tetracene MJ doped with a boron (B) atom, the localized LUMO is located within the tetracene molecule (i.e., a.), whereas in the event of a HOMO energy level, it is distributed throughout the junction (i.e., d.). The transport in this scenario need to be LUMO dominant. The situation is the opposite when a Nitrogen (N) atom is added to it. HOMO energy, or b., dominates the transit. The HOMO energy is LUMO dominated and well concentrated within the tetracene molecule (not on the anchoring group) when the junction is doped with both N and B atoms.

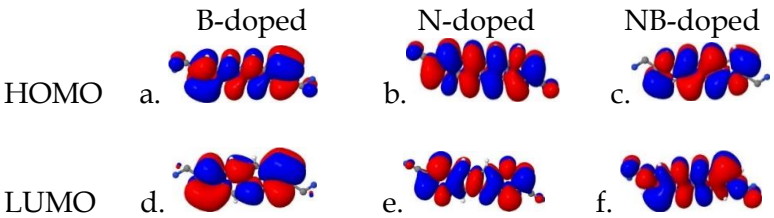

Figure 6: The frontier molecular orbitals of tetracene when doped with B, N and NB respectively

Table 3: HOMO-LUMO variation with impurity doping in tetracene MJs

Dopants	HOMO (eV)	LUMO (eV)	HOMO-LUMO gap(eV)
B	-4.7360	-4.6896	0.0464
N	-4.5677	-4.5476	0.0201
NB	-4.7012	-4.6882	0.0132

The Table 3 above shows that the NB-doped tetracene MJ has the minimum value of HOMO-LUMO gap, and it followed by N and B-doped respectively.

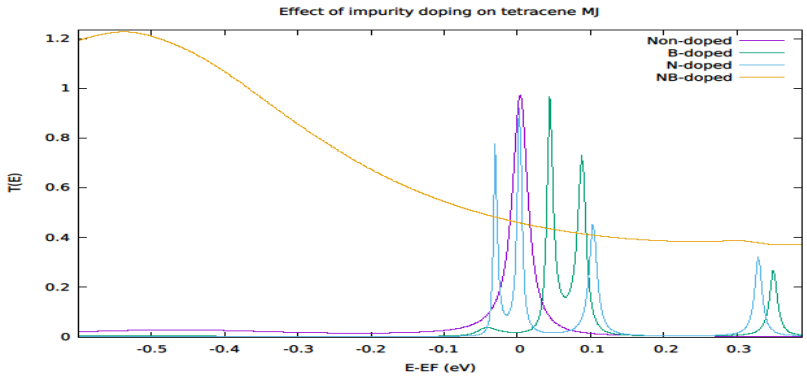

Figure 7: Transmission variation of tetracene MJ when doped with B, N and NB.

Figure 7 displays the transmission coefficients of B, N, and NB-doped tetracene MJs. The n-type (LUMO-dominated) transport feature is displayed by B-doped MJ, which has the lowest T(E) value of 0.1163 and a LUMO that is closer to Fermi energy (EF). The maximum T(E) of 0.6534 and a HOMO (i.e., p-type transport characteristic) that is closer to EF are also seen in the N-doped tetracene MJ. The T(E) value of NB-doped MJ is 0.4558, and its LUMO is nearer to E_F. Tetracene MJ's conductivity is decreased by N, B, and NB together. This is supported by Akbarabadi *et al.,* (2020).

3.2.2 Pentacene: B, N, and NB atoms were substituted with a single carbon here as well (Figure 8). B-dopant localizes the LUMO within the pentacene molecule with a HOMO-LUMO gap of 0.00148 eV and modifies the pentacene HOMO to resemble that of tetracene (see Figure 5a). With a HOMO-LUMO gap of 0.0061 eV, the N-dopant delocalizes the HOMO and partially localizes the LUMO within the pentacene molecule. On the other hand, NB-doped pentacene has a gap of 0.00139 eV and delocalizes the HOMO and partially localizes the LUMO within the molecule.

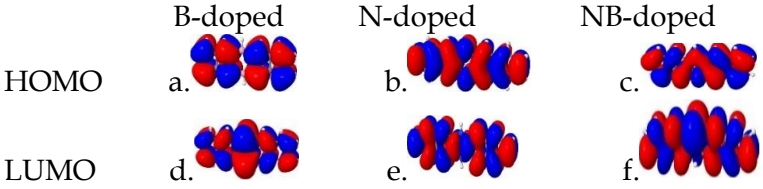

Figure 8: Frontier molecular orbitals of pentacene doped with B, N and NB respectively

Table 4: HOMO-LUMO variation with impurity doping

Doping	HOMO (eV)	LUMO (eV)	HOMO-LUMO gap(eV)
B-doped	-4.5851	-4.5836	0.00148
N-doped	-4.5085	-4.5024	0.0061
NB-doped	-4.5750	-4.5736	0.00139

Apart from the N-doped, all other dopants excites the tetracene MJs since their respective HOMO-LUMO gap reduces when doped.

The transmission coefficient T(E) of a pentacene MJ doped with N, B, and NB atoms is shown below (Figure 9). When these MJs are doped, their T(E) falls, indicating a decrease in conductance. The T(E) value at E_F is 0.000806 and the LUMO of pentacene MJ is closer to E_F (n-type transport) when it is doped with B atom (green). The HOMOs of N and NB-doped pentacene MJs are closer to E_F, indicating HOMO-dominated (p-type) transportation, with T(E) values of 0.02141 and 0.002133, respectively. This is in total agreement with Blanca and Blaze (2009).

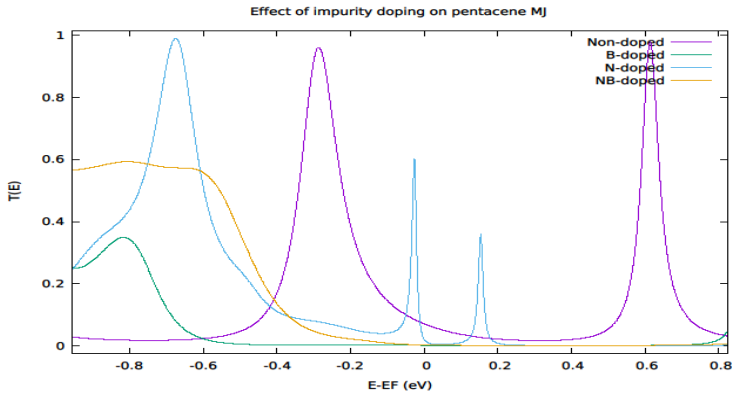

Figure 9: Transmission variation of pentacene MJ when doped with B, N and NB

Side Group: Thus far, four distinct anchoring groups and three impurity dopings have been examined. Now, the central benzene ring of the acene-based MJs will have three distinct side groups attached to it: amine (NH2), nitro (NO2), and methyl (CH3). According to Gil and Thijssen (2007), the introduction of a side group can control the alignment of HOMO or LUMO.

Tetracene MJs: The identical methyl (CH3), amine (NH2), and nitrate (NO2) side-groups were employed here as well. For the HOMO and LUMO energies, the side-groups had little effect on the tetracene MJs (see Figure 10) and primarily demonstrate a neutral transportation.

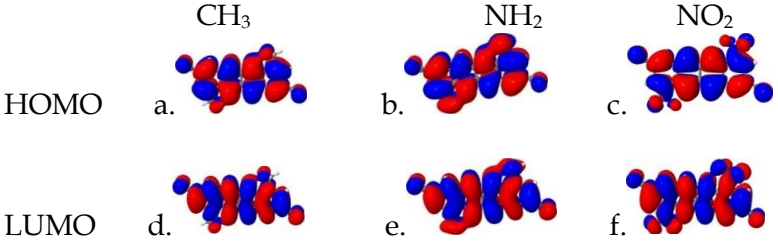

Figure 10: The frontier molecular orbitals for tetracene molecule with different side groups.

Table 5: HOMO and LUMO variations with different side groups in tetracene MJs

Side group	HOMO (eV)	LUMO (eV)	HOMO-LUMO gap (eV)
Methyl (-CH_3)	-4.7321	-4.7207	0.0114
Amines (-NH_2)	-4.6496	-4.6289	0.0207
Nitrates (-NO_2)	-4.9928	-4.9835	0.0093

Table 5, shows that when compared to unperturbed tetracene MJ (Table 2), all the side groups increases the value of HOMO-LUMO gap.

The transmission coefficients T(E) of tetracene MJs when they are disturbed by various side-groups are shown in Figure 11. The methyl (CH_3) side-group in this instance has the highest conductance value, with a T(E) value of 0.8761. The side-group of nitrates (NO_2), with a T(E) value of 0.6545, comes next. With the lowest conductance value when compared to the other side groups, the amines side-group (NH_2) has the lowest T(E) value of any of them.

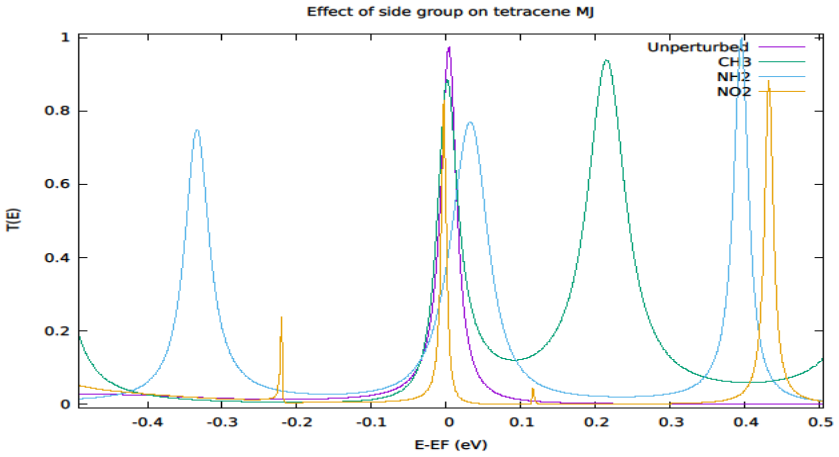

Figure 11: Transmission against energy for the transport in tetracene MJ with side-group

Pentacene: Here, methyl (CH_3) did not alter the structure of the HOMO and LUMO of the pentacene MJs (Figure 4a); instead, it reduced the gap to 0.0101 eV (see Table 6). Amines (NH_2) delocalized the HOMO and LUMO with a gap of 0.0108 eV, which is very close to that of the methyl. The nitrate (NO_2) group did not significantly alter the structures of the HOMO and the LUMO, but it did decrease the gap to 0.00572 eV, which means that it is easy to excite the pentacene MJs. Table 6 below displays the HOMO, LUMO, and energy gap of the pentacene MJs when they are perturbed with different side groups.

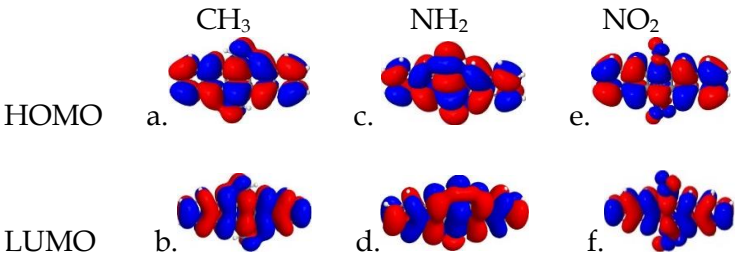

Figure 12: Frontier molecular orbitals for different side groups

Table 6: HOMO and LUMO variations of pentacene MJs with different side groups

Side group	HOMO (eV)	LUMO (eV)	HOMO-LUMO gap (eV)
Methyl (-CH_3)	-4.5489	-4.5388	0.0101
Amines (-NH_2)	-4.5439	-4.5331	0.0108
Nitro (-NO_2)	-4.7223	-4.7165	0.00572

Table 6 above shows the variation of HOMO-LUMO gap of a pentacene MJ with different side groups

Figure 13, below illustrates the transmission coefficients T(E) versus energy for the pentacene MJs when different side-groups were used. Side-groups increase the conductance of this type of junction; the highest T(E) value of this MJ at E_F when methyls are used (purple) as side-group is 0.3591, indicating a higher conductance value; this is followed by amines (green) and nitro (blue), with T(E) values of 0.3466 and 0.2365, respectively. This figure also demonstrates that all three of these cases exhibit p-type transport behaviors because their HOMOs are close to the Fermi energy (E_F). This is in total agreement with Vincent *et al.,* (2020).

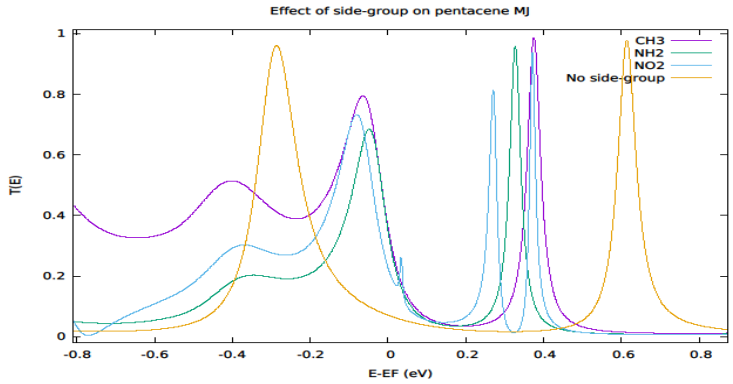

Figure 13: Transmission variation of pentacene MJ with side-groups

CONCLUSION

Acene-based MJs' electrical conductance was the focus of a theoretical analysis of their electronic transportation properties using DFT calculations and the NEGF formalism. First, research was done on the effects of anchoring groups like amines (NH_2), sulphides (S), cyanides (CN), and thiols (SH). The emphasis was on how each and every one of those anchoring groups alters the way an acene single molecule connection functions when it is coupled to gold electrodes. According to the data, amines with p-type transport, sulphides and thiols with p- and n-type transport capabilities, and cyanides anchor with the highest conductance value for tetracene MJs are the ones that follow. The order of the HOMO-LUMO gap is cyanides, sulfurides, amines, and thiols. Cyanides exhibit the highest conductance value among pentacene MJs, with n-type transport. Sulfides, on the other hand, have p-type transport, while amines have p-type transport features. Thiols have n-type transport features and the lowest conductance value. It also shows that the order of the HOMO-LUMO gap is sulfides, amines, cyanides, and thiols.

In addition, acene-based MJs were subjected to impurity doping, with B and N being employed as chemical dopants. According to the results, N-doped pentacene and tetracene MJs had the maximum conductance with p-type transport features, followed by NB- and B-doped pentacene and tetracene MJs with p- and n-type transport parameters, respectively. Tetracene MJs have a HOMO-LUMO gap in the order of NB<N<B, whereas pentacene MJs have a gap in the order of NB<B<N.

Finally, research was done on the impact of side groups such amine (NH_2), nitro (NO_2), and methyl (CH_3) on the conductance of acene-based MJs. The most conductance value (n-type) for tetracene MJs is methyl, followed by nitrates and amines, which have p- and n-type transport, respectively. The order of the HOMO-LUMO gap is NO_2<CH_3<NH_2. Methyl likewise has the maximum conductivity value in the case of pentacene MJs, followed by amines and nitrates, in that order. Here, each of these side groups resulted in a p-type (HOMO-dominated) transport behavior. The order of the HOMO-LUMO gap is NO_2<CH_3<NH_2.

Acknowledgments
We want to acknowledge the effort of Professor A. S. Gidado for the helpful discussions and professional advice. We also show our appreciation to Professor M. A. Hajara for the spotlight in the field of Electronics.

References

Aadhityan, A., Preferencial, K. C., and John, T. D. (2020). Theoretical Investigation of Spin-dependent Electron Transport Properties of Dibromobenzene based Positional Isomers. *Computational Matt. Sci.,* 15, 0927-0956.

Ali, K. I., Alaa, A. J., Iain, G., and Colin, J. L. (2017). Discriminating single-molecule sensing by crown-ether-based molecular junction. *THE JOURNAL OF CHEMICAL PHYSICS*, 0647041-0647045.

Akbarabadi, S.R., Soleimani, H.R., Golsanamlou, Z., and Tagani, M.B. (2020). Enhanced thermoelectric properties in anthracene molecular device with graphene electrodes: the role of phononic thermal conductance. *Scientific Reports.* 10, 10922.

Akbarabadi, S.R., Soleimani, H.R. and Tagani, M.B. (2021). Side-group-mediated thermoelectric properties of an anthracene single-molecule junction with anchoring groups. *Scientific Reports.* 11, 8958.

Arnold, A., Weigend, F., and Evers, F. (2007). Quantum chemistry calculations for molecules coupled to reservoirs: Formalism, implementation, and application to benzenedithiol. *The Journal of Chemical Physics.*, 174101-12.

Aviram, A. and Ratner, M. A. (1974). Molecular Rectifiers. *Chemical Physics Letters,* 29, 277.

Bagrets, A. (2013). Spin-polarized electron transport across metal-organic molecules: a density functional theory approach. *Journal of Chemical Theory and Computation*, 2801-45.

Balachandran, J., Reddy, P., Dunietz, B.D. and Gavini, V. (2012). End-Group-Induced Charge Transfer in Molecular Junctions: Effect on Electrinic-Structure and Thermopower. *Physical Chemistry Letters.* 3, 1962-1967.

Blanca B. X. and Blasé F. T. (2009). Anomalous Doping Effects on Charge Transport in Graphene Nanoribbons. *Phys. Rev. Lett.,* 102, 096803.

Blum, V., Gehrke, R., Hanke, F., Havu, P., Havu, V., Ren, X., and Reuter, M. S. (2009). Ab initio molecular simulations with numeric atom-centered orbitals. *Computer Physics Communications*, 2175-2196.

Chen, H. L., Zheng, H. N., Hu, C., Cai, K., Jiao, Y., Zhang, L., Jiang, F., Roy, I., Qiu, Y. Y., Shen, D. K., Feng, Y. N.,Hong, W. and Stoddart, J. F. (2020). *Matter*, 2, 278.

Cheng, N., Liuyue, Z., Colm, D., Nan, W., Binyang, D., Jianwei, Z., and Yuanyuan, H. (2020). Electron Transport through a Coordination Junction Formed by Carboxy Thiophenols and Bivalent Metal Ions. *The Journal of Physical Chemistry*, 21137-21146.

Fujii, S., Madoka, I., Shunsuke, F., Tomofumi, T., Tomoaki, N., Masaichi, S., and Manabu, K. (2020). Hybrid Molecular Junctions Using Au-S and Au-π Bindings. *The Journal of Physical Chemistry C*, 9261-9268.

Gil, C. J., and Thijssen, J. M. (2017). Transport gap renormalization at a metal-molecule interface using DFT-NEGF and spin unrestricted calculations. *The Journal of Chemical Physics*, 0841021-0841028.

He, C., Zhang, Q., Gao, T., Liu, C., Chen, Z., Zhao, C., Nichols, R. J., Dappe, Y. and Yang, L. (2020). Charge Transport in Hybrid Platinum/Molecule/Graphene Single Molecule Junctions. *Phys. Chem. Chem. Phys.*, DOI: 10.1039/D0CP01774D

Ibrahim, K. L., Babaji G. and Nura A. M. (2022). Charge Transport Enhancement in Anthracene Molecular Junction: Density Functional Theory Studies. *J. Mater. Sci. Res. Rev.,* vol. 10, no. 4, pp. 32-41, 2022; Article no.JMSRR.95693.

Michael, T., and Ferdinand, E. (2018). Perspective: Theory of quantum transport in molecular junctions. *The Journal of Chemical Physics, 148*, 1-16.

Noori, M. D., Sangtarash, S. and Sadeghi, H. (2021). The effect of anchor group on the phonon thermal conductance of single molecule junctions. *Appl. Sci.* 11, 1066.

Pinheiro, M., Machada, F.B.C., Plasser, F., Aquino, J.A., and Lischka, H. (2020). A system analysis of excitonic properties to seek optimal singlet fission: the BN-substitution patterns in tetracene. *Journal of Material Chemistry C.* (DOI: 10.1039/C9TC06581D).

Ramezani, A. S., Rahimpour, S. H., and Bagheri, T. M. (2021). Side-group-mediated thermoelectric properties of anthracene single-molecule junction with anchoring groups. *Sci. Rep.* 11, 1, 8958. DOI: 10.1038/s41598-021-88297-2.

Sirohi, A., SanthiBhushan, B., and Srivastava, A. (2021). Charge transport in polythiophene molecular device: DFT analysis. *Journal of molecular modeling,* 27:77. https://doi.org/10.1007/s00894-021-04680-w

Stegmann, T., Franco-Villafane, J. A., Ortiz, Y. P., Deffner, M., Herrman, C., Kuhl, U., . . . Seligman, T. H. (2020). Current vortices in aromatic carbon molecules. *Physical Review B*, 075405-1-10.

Vincent, D., Valentin, D. C., Colin, V. D., ELke, S., Karine, C., and Jerome, C. (2020). On the reliability of acquiring molecular junction parameters by Lorentzian fitting I/V curved. *Royal Society of Chemistry*, 1-5.

Wang, Y., Huang, H., Yu, Z., Zheng, J.-F., Shao, Y., Zhou, X.-S., . . . Li, J.-F. (2020). Modulating electron transport through single-molecule junctions by heteroatom subtitution. *Journal of Materials Chemistry C*, 1-7.

Wilhelm, J., Walz, M., Stendel, M., Bagrets, A., and Evers, F. (2013). Ab initio simulations of scanning-tunneling-microscope images with embedding techniques and application to C58-dimers on Au(111). *Phys. Chem. Chem. Phys.*, 6684-6690.

Yelin T., Chakrabarti S, Vilan A., Tal O. (2021). Richness of molecular junction configurations revealed by tracking a full pull-push cycle. *Nanoscale* , **13**, 18434-18440. DOI: https://doi.org/10.1039/D1NR05680H

Yuan, S., Gao, T., Cao, W., Pan, Z., Liu, J., Shi, J., Hong, W. (2021). The characterization of electronic noise in the charge transport through single-molecule junctions. *Small Methods,* 5, 2001064. DOI: 10.1002/smtd.202001064.